Reaction kinetics of diffusing particles injected into a reactive substrate

A. D. Sánchez,* S. Bouzat,† and H. S. Wio‡
Centro Atómico Bariloche (CNEA) and Instituto Balseiro (CNEA and UNC), 8400-San Carlos de Bariloche, Argentina
(Received 2 February 1999)

We analyze the kinetics of trapping ($A+B\rightarrow B$) and annihilation ($A+B\rightarrow 0$) processes on a one-dimensional substrate with homogeneous distribution of immobile B particles while the A particles are supplied by a localized source. For the imperfect reaction case, we analyze both problems by means of a stochastic model and compare the results with numerical simulations. In addition, we present the exact analytical results of the stochastic model for the case of perfect trapping. [S1063-651X(99)08509-8]

PACS number(s): 82.20.Wt, 02.50.−r

I. INTRODUCTION

The dynamics of diffusion-controlled reactions has been extensively studied in recent years due to its relevance in the most diverse areas of physics, chemistry, and biology [1]. These studies include trapping, coalescence and annihilation of one and two species, corresponding to assorted processes in heterogeneous reactions, catalysis, or membrane processes in biology. It is of great interest to find theoretical models that correctly describe the different possible situations as the usual mean-field (MF) description fails when the system dimension d is low ($d\leqslant 2$). Since the first contributions of Smoluchowski [2], many different models have been proposed [1,3], trying to include aspects related with fluctuations and correlations, but with limited success.

Recently, and in order to obtain a better description of trapping ($A+B\rightarrow B$) as well as annihilation ($A+B\rightarrow 0$) reactions, a stochastically based model was introduced [4–7]. The equation for the evolution of the densities in such a model, corresponding to the continuous limit of the master equation describing the simulations, has been successful in describing several related situations, showing a very good agreement with numerical simulations. Such a framework also offers an adequate description for short, intermediate and long-time regimes. This model has been extended to different situations corresponding to quasidynamical traps [8], existence of sources [9], behavior of the reaction front for initially separate reactants [10], nearest-neighbor distances [11], and coupled reactions (or trapping with a time-dependent number of traps) [12].

An annihilation problem that has been studied through experiments, theory, and simulations [13–20], corresponds to the case in which the reactants are initially separated in space. In this situation, the theoretical analysis of the behavior of the reaction front is done in terms of one-dimensional reaction-diffusion equations where the reaction terms are modeled according to chemical kinetics [13–18]. Recently, renormalization-group techniques have also been used, starting from a master equation describing the process and transforming it into a second quantized version [21]. In Refs. [10,20] a different and more accessible framework has been used, which is based on the stochastic model (SM) indicated above. Within such a framework, scaling relations for the form of the fronts have been obtained, with exponents that agree with those obtained in recent simulations [19]. An experimental realization of this one-dimensional annihilation problem is due to Koo and Kopelman [15], corresponding to a reaction performed in a capillary.

In this paper we consider two related problems, trapping and annihilation in a one-dimensional system with a localized constant source of diffusing particles A, and the particles B uniformly distributed and immobile. We have made a theoretical analysis of each problem using the SM and also the simple MF description, and compared all the results with numerical simulations. Associated experiments could be performed by implementing appropriate modifications of the experimental arrangement of Koo and Kopelman [15]. The experimental configuration would consist of a ''T-like'' capillary structure, with the A particles injected at a constant rate through the vertical branch of the ''T,'' while the B's are located in the horizontal branch.

Two papers that deal with closely related problems of reactions in the presence of a localized source are those in Refs. [9,22]. In Ref. [9] the trapping problem with periodically distributed traps was analyzed by means of the SM and the results compared with simulations. In Ref. [22] the perfect annihilation problem was theoretically studied by means of a diffusion equation with a mobile boundary and simulations, and experimental results were presented as well.

The organization of the paper is as follows. We first study the imperfect trapping problem presenting analytical solutions for the SM (approximate) and MF models, and also discuss some scaling properties. Then we present the exact solutions of the SM for the cases of perfect trapping reactions in infinite and finite substrates. All results are compared with numerical simulations. Next, we numerically analyze the solutions of the SM and MF model for the case of imperfect annihilation and compare them with simulations. The last section is devoted to our conclusions.

II. TRAPPING REACTIONS

We analyze a system consisting of a one-dimensional substrate with a uniform density of fixed B particles, and a localized source of diffusive A particles. The particles undergo

*Electronic address: sanchez@cab.cnea.gov.ar
†Electronic address: bouzat@cab.cnea.gov.ar
‡Electronic address: wio@cab.cnea.gov.ar

a trapping process $A+B\rightarrow B$. As the initial condition we take a null density of A particles.

The MF equation for the density of A particles $n_A(x,t)$ is

$$\frac{\partial n_A(x,t)}{\partial t}=D\frac{\partial^2 n_A(x,t)}{\partial x^2}-\gamma n_B n_A(x,t)+n_p\delta(x), \quad (1)$$

where n_B is the (constant) density of traps, D is the diffusivity of A particles, γ is the reaction rate, and n_p is the intensity of the source (number of particles injected per unit time). The Laplace–Fourier transform of this equation, given by

$$n_A(k,s)=\frac{n_p}{s(s+Dk^2+\gamma n_B)}, \quad (2)$$

can be inverted to obtain the exact solution

$$n_A(x,t)=\frac{n_p}{2\sqrt{\gamma n_B D}}\left[e^{-a|x|}-\frac{1}{2}e^{-ax}\mathrm{erfc}\left(a\sqrt{Dt}-\frac{x}{2\sqrt{Dt}}\right)-\frac{1}{2}e^{ax}\mathrm{erfc}\left(a\sqrt{Dt}+\frac{x}{2\sqrt{Dt}}\right)\right], \quad (3)$$

where $a=\sqrt{\gamma n_B/D}$. By integration we obtain $N_A(t)$, the number of surviving particles at a given time, given by

$$N_A(t)=\int_{-\infty}^{\infty}n_A(x,t)dx=\frac{n_p}{\gamma n_B}[1-\exp(-\gamma n_B t)]. \quad (4)$$

We now consider the SM [5]. The basic equation of the model is

$$\frac{\partial \rho_A(x,t)}{\partial t}=D\frac{\partial^2 \rho_A(x,t)}{\partial x^2}-\gamma\sum_i \delta(x-R_i)\rho_A(x,t)+n_p\delta(x), \quad (5)$$

where the R_is are the random (uniformly distributed) positions of the traps and ρ_A is the A density for a given realization of the process. The actual density is given by the ensemble average $n_A(x,t)=\langle\rho_A(x,t)\rangle$.

The average was performed by a procedure similar to the one used in [5], involving several approximations. The result for the Laplace-Fourier transform of the (approximated) density, is

$$n_A(k,s)=\frac{n_p}{s+Dk^2}\left[\frac{1}{s}-\frac{\gamma n_B}{(s+Dk^2)\left(s+\gamma\sqrt{\frac{s}{4D}}\right)+\gamma n_B s}\right]. \quad (6)$$

Taking the inverse Fourier–Laplace transform of Eq. (6) is a very difficult task; hence, we only calculate the number of surviving particles, which can be obtained from the inverse Laplace transform of $n_A(k=0,s)$, resulting in

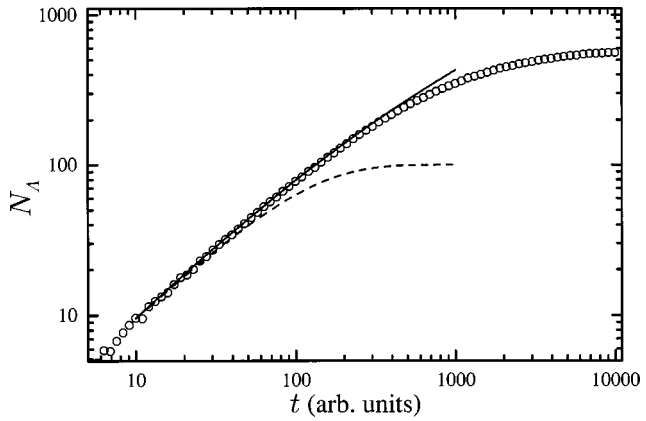

FIG. 1. Temporal evolution of the number of surviving A particles in an imperfect trapping reaction. The solid line corresponds to the results of the SM, the dashed line corresponds to MF results, and the dots correspond to numerical simulations. The parameters used are $D=\gamma=n_B=0.1$ and $n_p=1$. Numerical simulations have been performed on a latice of 1000 sites.

$$N_A(t)=n_p t-\frac{n_p\gamma n_B}{\nu_+-\nu_-}\left[\left(\frac{1}{\nu_-^3}-\frac{1}{\nu_+^3}\right)+\left(\frac{1}{\nu_-^2}-\frac{1}{\nu_+^2}\right)\times\sqrt{\frac{4t}{\pi}}+\left(\frac{1}{\nu_-}-\frac{1}{\nu_+}\right)t+\frac{1}{\nu_+^3}e^{\nu_+^2 t}\times\mathrm{erfc}(-\nu_+\sqrt{t})-\frac{1}{\nu_-^3}e^{\nu_-^2 t}\mathrm{erfc}(-\nu_-\sqrt{t})\right], \quad (7)$$

where $\nu_\pm=-\gamma(/4\sqrt{D})\pm\sqrt{\gamma^2/(16D)-n_B\gamma}$. We note that Eq. (7) only depends on two parameters: $\gamma/\sqrt{D}$ and $n_B\gamma$. From Eq. (6) it is also possible to obtain the scaling properties of the spatially dependent solution. Hence, we have

$$\frac{n_A(x,t)}{n_p/\sqrt{D}}=f_1(\gamma n_B,\gamma/\sqrt{D},t,x^2/D), \quad (8)$$

$$\frac{N_A(t)}{n_p}=f_2(\gamma n_B,\gamma/\sqrt{D},t). \quad (9)$$

In Fig. 1 we compare the results for $N_A(t)$ of the MF approach and of the SM with numerical simulations. It can be observed that the (approximated) solution found for the SM shows good agreement with data from simulations for longer times than the (exact) solution of the MF model. For $t\rightarrow\infty$ neither of the solutions describes the simulations correctly: while the solution of the SM diverges, MF results predict an incorrect final value. The discrepancy of exact MF results reveals an intrinsic feature of the model, which is its well-known incapability of taking into account segregation effects, which leads to an overestimation of the absorption. On the other hand, the differences between the SM solution and simulations are due to the approximations made in order to obtain Eq. (6).

At variance of the approximated solutions, the scaling relations emerging from the SM turn out to be valid for all times (at least to a very good approximation) as can be seen in Fig. 2. In Fig. 2(a) we show results from simulations for

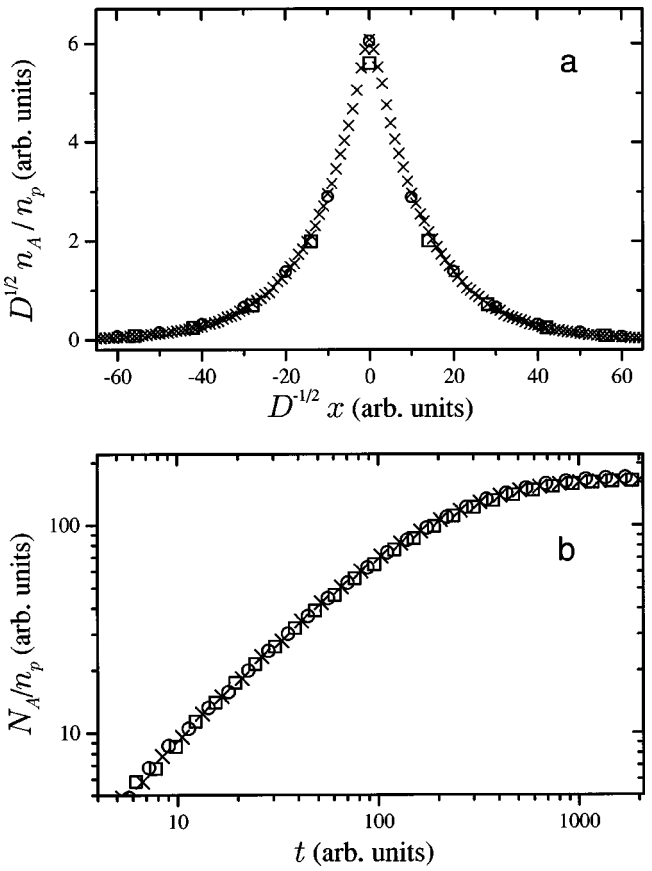

FIG. 2. Results from simulations for distribution of A particles at $t=2000$ (a) and for the temporal evolution of the number of surviving A particles (b), for different sets of parameters: $n_B=0.1$, $D=1$, $\gamma=0.1$, $L=250$, 5000 realizations (crosses), $n_B=1$, $D=0.01$, $\gamma=0.01$, $L=200$, 10 000 realizations (circles), $n_B=1.4$, $D=0.0051$, $\gamma=0.0071$, $L=50$ and 10 000 realizations (squares) with $n_p=1$ for all sets. Note that if the scaling given by Eqs. (8) and (9) is valid, all the simulations must be coincident since they all have $\gamma n_B=0.01$ and $\gamma D^{-1/2}=0.1$.

the spatial distribution of A for three sets of parameters related through the scaling property emerging from Eq. (8). The curves correspond to a time for which the system has reached its stationary regime and the scaling is still valid. Similar results for earlier times are as good as those just shown. From Fig. 2(b) it can be seen that the scaling for $N_A(t)$ given by Eq. (9) is also valid. Hence from the SM we have obtained not only an approximate solution valid for short and intermediate times, but also scaling relations valid for all times. It is worth mentioning that the scaling relations emerging from the exact solution of the MF model are only valid for very short times (those where such a solution correctly describes simulations).

In contrast with the case of imperfect reactions we can solve the SM exactly when perfect reactions are considered. It is worth remarking that the MF model gives a null density, as can be seen taking the limit $\gamma\to\infty$ in Eq. (4). The solution for the SM can be obtained noting that, in a given realization, only two traps (those closest to the source on each side of it) are significant in the problem due to the fact that the density is zero outside of the interval between them. Then we can write the expression for the density if the trap on the left is at $x=-x_0$ and the trap on the right is at $x=x_1$, by solving the diffusion equation with absorbent conditions at $-x_0$ and x_1, giving

$$\frac{\rho_A(x_0,x_1,x,t)}{n_p}=\sum_{j=-\infty}^{\infty}\left\{\sqrt{\frac{t}{\pi D}}e^{-[x-2j(x_0+x_1)]^2/4Dt}-\frac{|x-2j(x_0+x_1)|}{2D}\times\mathrm{erfc}\left(\frac{|x-2j(x_0+x_1)|}{\sqrt{4Dt}}\right)-\sqrt{\frac{t}{\pi D}}e^{-[x-2(j-1)x_0-2jx_1]^2/4Dt}+\frac{|x-2(j-1)x_0-2jx_1|}{2D}\times\mathrm{erfc}\left(\frac{|x-2(j-1)x_0-2jx_1|}{\sqrt{4Dt}}\right)\right\}, \tag{10}$$

for $-x_0<x<x_1$ and zero otherwise. This equation is a sum of densities corresponding to an infinite number of images that must be alternately added and subtracted to obtain a null value of the actual density at both trap positions. The following step is averaging over the trap positions x_0 and x_1. For $x>0$ we have

$$n_A(x,t)=\int_0^\infty dx_0\int_x^\infty dx_1\rho_A(x_0,x_1,x,t)n_B^2\times\exp[-n_B(x_0+x_1)]. \tag{11}$$

For $x<0$ the solution can be obtained by reflection. The x in the lower limit of the integral over x_1 takes into account that the density is zero beyond x_1. After a tedious calculation, the average is found to be

$$\frac{n_A(x,t)}{n_p}=\frac{1}{n_BD}e^{-n_B|x|}\mathrm{erfc}\left(\frac{|x|}{\sqrt{4Dt}}\right) \tag{12}$$

$$-\frac{1}{n_BD}e^{(n_B/4)(Dn_Bt-2|x|)}\mathrm{erfc}\left(\frac{|x|+Dn_Bt}{\sqrt{4Dt}}\right)+\sum_{j=-\infty,\neq 0}^{\infty}\sqrt{\frac{t}{\pi D}}e^{-[4Dn_Bt+(2j-1)^2|x|]|x|/(4Dt)}+\mathrm{sgn}(j)\left\{-\frac{1}{n_BD}e^{-n_B|x|}\mathrm{erfc}\left(\frac{|2j-1||x|}{\sqrt{4Dt}}\right)-\left[\frac{j(j-2)}{n_BD}+\frac{n_Bt}{2j}+\frac{(2j-1)|x|}{2D}\right]\times e^{(Dn_Bt-2j|x|)n_B/(4j^2)}\mathrm{erfc}\left(\frac{Dn_Bt+j(2j-1)|x|}{|j|\sqrt{4Dt}}\right)\right.$$

$$+\frac{(j-1)^2}{Dn_B}e^{[Dn_Bt+2(j-1)|x|]n_B/[4(j-1)^2]}$$
$$\times\mathrm{erfc}\left(\frac{Dn_Bt+(j-1)(2j-1)|x|}{|j-1|\sqrt{4Dt}}\right)\Bigg\}.$$

The number of particles can be obtained by integration, yielding

$$\frac{N_A(t)}{n_p}=\frac{4}{n_B}\sqrt{\frac{t}{\pi D}}-\frac{4}{Dn_B^2}e^{(1/4)Dn_B^2t}\mathrm{erfc}\left(\frac{1}{2}n_B\sqrt{Dt}\right)$$
$$+\frac{2}{Dn_B^2}e^{Dn_B^2t}\mathrm{erfc}(n_B\sqrt{Dt})+2\sum_{j=-\infty}^{\infty}\mathrm{sgn}(j)$$
$$\times\left\{\frac{(2j-1)^3}{Dn_B^2}e^{Dn_B^2t/(2j-1)^2}\mathrm{erfc}\left(\frac{n_B\sqrt{Dt}}{|2j-1|}\right)\right.$$
$$-2\frac{(j-1)^3}{Dn_B^2}e^{Dn_B^2t/(j-1)^2}\mathrm{erfc}\left(\frac{n_B\sqrt{Dt}}{2|j-1|}\right)$$
$$\left.-6\frac{j^3}{Dn_B^2}e^{Dn_B^2t/(4j^2)}\mathrm{erfc}\left(\frac{n_B\sqrt{Dt}}{2|j|}\right)\right\}. \quad (13)$$

The last equation depends on two parameters, D and n_B, only through the combination n_B^2D, which remains as the only relevant parameter.

Although general expressions (12) and (13) are valid for all times, a compact expression can be obtained in the asymptotic regime. Such expressions can be derived noting that a stationary density is asymptotically reached. Then, for a given realization, the density profile is composed of two straight lines from the source to each trap, where it is zero (the reason for this is described in Ref. [9]). By making a balance between the diffusive current and the particles supplied by the source the density at the origin

$$n_A(0,t\to\infty)=\frac{n_p}{D}\frac{x_0x_1}{x_0+x_1}. \quad (14)$$

Then, proceeding in a similar way as before, we perform the averaging, to obtain

$$n_A(x,t\to\infty)=\frac{n_p}{Dn_B}E_4(n_B|x|), \quad (15)$$

$$N_A(t\to\infty)=\frac{n_p}{2D}\frac{1}{n_B^2}, \quad (16)$$

where $E_n(x)$ denotes the exponential integral function of order n [23].

As the SM was exactly solved we expect a very good agreement between theory and simulations, as in previous cases where exact solutions were obtained [5,8,9,11]. In Fig. 3 we show results from simulations and theory for the density profiles at two different times [Fig. 3(a)] and for the number of particles [Fig. 3(b)]. The small discrepancy between circles and the solid line in Fig. 3(b) is a consequence of describing a discrete system by a continuous model and of

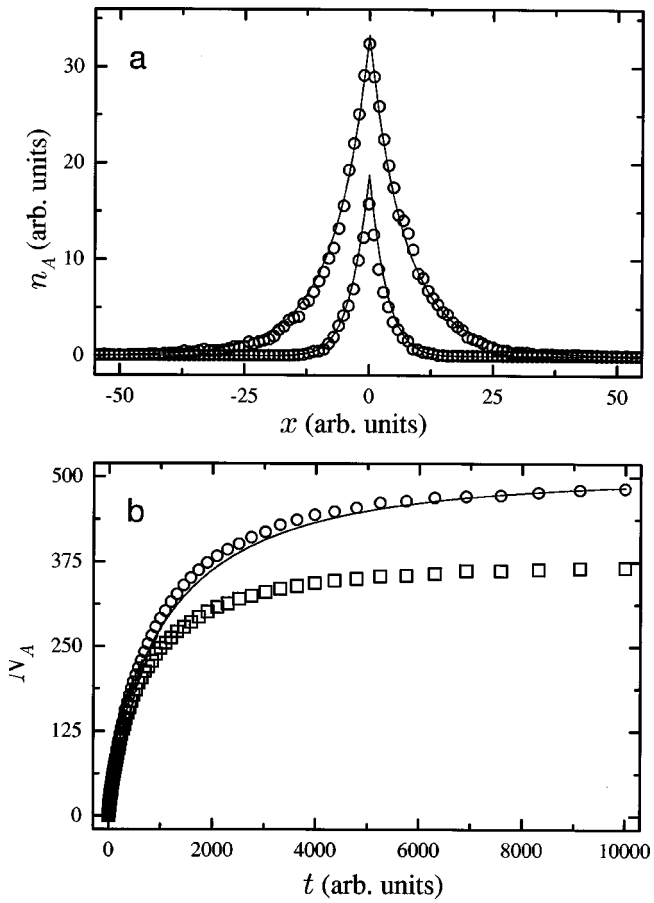

FIG. 3. Density profile (a) and number of surviving A particles (b) for a perfect trapping reaction. In (a) density profiles correspond to $t=10\,000$ (top) and $t=250$ (bottom). The solid lines correspond to SM results for stationary profile [Eq. (15)] and for $t=250$ [10 terms in the sum of Eq. (12)] while dots are the result of numerical simulations. In (b) the solid line corresponds to results for an infinite lattice [20 terms in the sum of Eq. (13)] and the dots correspond to numerical simulations. The final value corresponding to the finite-size calculation given by Eq. (21) is $N_A(t\to\infty)=485.3$ (circles) and 378.8 (squares), while the $L\to\infty$ value given by Eq. (16) is $N_A(t\to\infty)=500$. The parameters used are $n_p=1$ and $n_B=D=0.1$. Numerical simulations have been made on a lattice of 1000 sites (circles) or 100 sites (squares).

finite-size effects. Concerning simulations we note that the condition of no particles reaching the boundaries of the lattice is not sufficient to prevent finite-size effects. This is because the exponential distribution of x_0 and x_1 used in Eq. (11) is valid only for an infinite lattice. Simulations using not large enough lattices produce lower densities because realizations where traps are very far from the source are excluded. This effect is apparent in the figure (squares) since the width of the density profile is smaller than the lattice length.

In a theory of finite lattices with periodic boundary conditions the averages of Eq. (10) must be taken using the adequate joint probability distribution function for x_0 and x_1 (which for finite L are not independent variables) that is given by

$$p(x_0;x_1)=\frac{N_B(N_B-1)}{L^2}\left(1-\frac{x_0+x_1}{L}\right)^{N_B-2}, \quad (17)$$

where L is the lattice length and N_B is the number of traps. The average is given now by

$$n_A(x,t)=n_A^*(|x|,t)+n_A^*(L-|x|,t), \tag{18}$$

where

$$n_A^*(x,t)=\int_x^L dx_1\int_0^{L-x_1} dx_0 p(x_0;x_1)\rho_A(x_0,x_1,x,t). \tag{19}$$

Although an analytical expression for $n_A(x,t)$ may be obtained, this would be rather complex, involving multiple sums of incomplete gamma functions. We only quote here the stationary solutions for density and particle number, that are given by

$$\begin{aligned}\frac{D}{n_p}n_A^*(x,t\to\infty)=&\frac{1}{3}\frac{1}{n_B+\frac{1}{L}}-\frac{1}{2}x+\frac{1}{2}n_Bx^2\\&+\frac{1}{6}n_B\left(n_B-\frac{1}{L}\right)x^3\left[\ln\left(\frac{x}{L}\right)-\frac{11}{6}\right]\\&+\sum_{i=1}^{N-2}\frac{N!}{(N-i-2)!}\frac{(-1)^i}{i}\frac{x^3}{L^2}\\&\times\left[\frac{1}{(i+3)!}\left(\frac{x}{L}\right)^i-\frac{1}{6i!}\right],\end{aligned} \tag{20}$$

$$N_A(t\to\infty)=\frac{n_p}{2D}\frac{1}{\left(n_B+\frac{1}{L}\right)\left(n_B+\frac{2}{L}\right)}. \tag{21}$$

Finally, an interesting fact to mention about trapping reactions is that the solution of the SM for the problem of many A particle sources localized at arbitrary positions is simply the sum of the solutions for the problem of one source at each position.

III. ANNIHILATION REACTIONS

Here we analyze a system consisting of a one-dimensional substrate with a uniform initial density n_{B0} of fixed B particles, and a localized source of diffusive A particles. The particles undergo an annihilation reaction $A+B\to 0$. Again, we consider a null initial density of A particles. We will analyze only the case of imperfect reactions, since that of a perfect reaction was analyzed by Larralde *et al.* in [22].

The equations of the MF model are

$$\frac{\partial n_A(x,t)}{\partial t}=D\frac{\partial^2 n_A(x,t)}{\partial x^2}-\gamma n_A(x,t)n_B(x,t)+n_p\delta(x), \tag{22a}$$

$$\frac{\partial n_B(x,t)}{\partial t}=-\gamma n_A(x,t)n_B(x,t), \tag{22b}$$

with initial conditions $n_A(x,0)=0$ and $n_B(x,0)=n_{B0}$. In dimensionless variables they become

$$\frac{\partial \tilde{n}_A(\tilde{x},\tilde{t})}{\partial \tilde{t}}=\tilde{D}\frac{\partial^2 \tilde{n}_A(\tilde{x},\tilde{t})}{\partial \tilde{x}^2}-\tilde{\gamma}\tilde{n}_A(\tilde{x},\tilde{t})\tilde{n}_B(\tilde{x},\tilde{t})+\delta(\tilde{x}), \tag{23a}$$

$$\frac{\partial \tilde{n}_B(\tilde{x},\tilde{t})}{\partial \tilde{t}}=-\tilde{\gamma}\tilde{n}_A(\tilde{x},\tilde{t})\tilde{n}_B(\tilde{x},\tilde{t}), \tag{23b}$$

with $\tilde{x}=xn_{B0}$, $\tilde{t}=tn_p$, $\tilde{n}_A=n_A/n_{B0}$, $\tilde{n}_B=n_B/n_{B0}$, $\tilde{D}=Dn_{B0}^2/n_p$, $\tilde{\gamma}=\gamma n_{B0}/n_p$, and the initial conditions $\tilde{n}_A(\tilde{x},0)=0$ and $\tilde{n}_B(\tilde{x},0)=1$. Hence only two parameters remain, namely, $\tilde{\gamma}$ and $\tilde{D}$.

The SM can also be used to describe this problem of annihilation with a source, the general procedures being like those in [6]. Within the so-called *sudden* approximation [6], we obtain the following (dimensionless) equations for the densities, averaged over all possible annihilation processes,

$$\begin{aligned}\frac{\partial \tilde{n}_A(\tilde{x},\tilde{t})}{\partial \tilde{t}}=&\tilde{D}\frac{\partial^2 \tilde{n}_A(\tilde{x},\tilde{t})}{\partial \tilde{x}^2}+\delta(\tilde{x})\\&-\tilde{\gamma}\int_0^{\tilde{t}}dt'\int_{-\infty}^{\infty}dx'T(\tilde{x}-x',\tilde{t}-t')\\&\times\tilde{n}_B(x',t')\tilde{n}_A(x',t'),\end{aligned} \tag{24a}$$

$$\begin{aligned}\frac{\partial \tilde{n}_B(\tilde{x},\tilde{t})}{\partial \tilde{t}}=&-\tilde{\gamma}\int_0^{\tilde{t}}dt'\int_{-\infty}^{\infty}dx'T(\tilde{x}-x',\tilde{t}-t')\\&\times\tilde{n}_A(x',t')\tilde{n}_B(x',t'),\end{aligned} \tag{24b}$$

where $T(x,t)=\delta(x)[\eta^2\exp(\eta^2 t)\mathrm{erfc}(\eta\sqrt{t})-\eta/\sqrt{\pi t}+\delta(t)]$, with $\eta=\tilde{\gamma}/\sqrt{4\tilde{D}}$.

The expressions for the number of particles in dimensionless and dimensional variables are related through

$$\begin{aligned}\tilde{N}_A(\tilde{t})=\int_{-\infty}^{\infty}\tilde{n}_A(\tilde{x},\tilde{t})d\tilde{x}=&\int_{-\infty}^{\infty}n_A(x,t)dx|_{t=\tilde{t}/n_p}\\=&N_A(t)|_{t=\tilde{t}/n_p}.\end{aligned} \tag{25}$$

The numerical solutions of Eqs. (23) and (24) are coincident and show excellent agreement with simulations. Thus, both models correctly describe the dynamics of the problem. However, as the MF results have a lower computational cost we will only show those corresponding to this model.

In Fig. 4 we show the numerical solutions of the MF model for the density profiles together with results of numerical simulations. We see that in spite of what happens with the MF model in the trapping problem, here the agreement is excellent. As the MF treatment usually gives incorrect results in similar problems (in dimensions below 2), this surprising fact can be understood as a consequence of the lack of segregation. In fact, in the case of annihilation without sources with uniform initial densities, the MF model fails in describing the temporal evolution due to the occurrence of the well-known segregation phenomenon, which leads to the formation of one species islands. However, in the present problem the islands are extremely rare (as can be seen from simulations observing single realizations), since it is too dif-

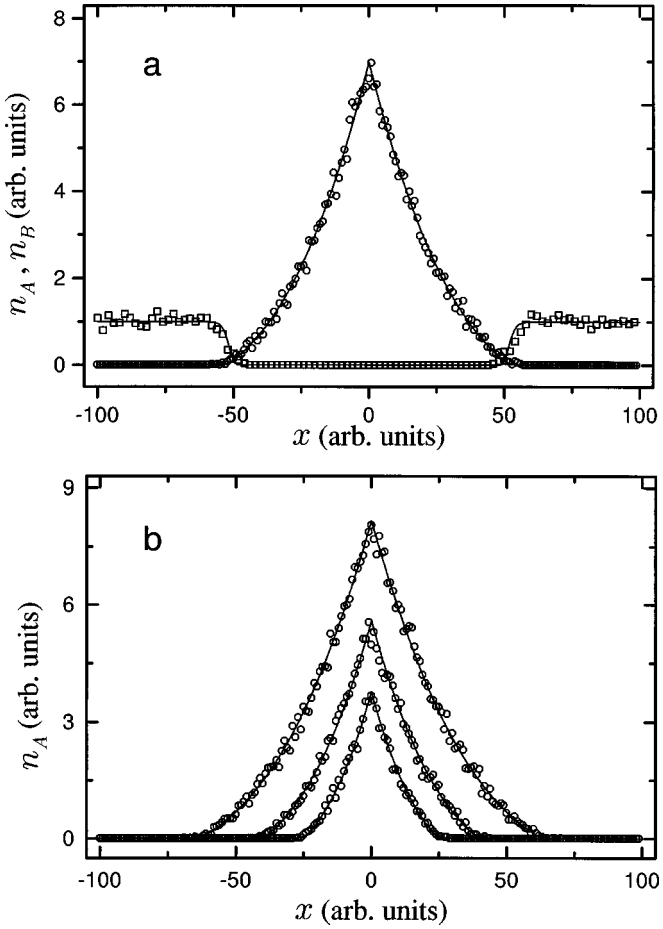

FIG. 4. Density profiles for imperfect annihilation reactions for $\gamma = n_{B0} = n_p = 1$ and $D = 2$. Solid lines correspond to MF results and dots correspond to simulations ($L = 200$). (a) Density profiles for $t = 375$. Circles correspond to A particles and squares correspond to B particles. (b) Distribution of A particles corresponding (from top to bottom) to $t = 500$, 250, and 125.

ficult for the A particles to penetrate the region rich in B particles without being annihilated.

Figure 5 shows the temporal evolution of the number of particles for two different sets of parameters. The excellent agreement between MF results and simulations is apparent. It can be seen that, for a given time, $N(t)$ decreases as $\tilde{D}$ is increased. This is because, with stronger diffusion, the A particles can reach regions farther from the source and meet a larger number of B particles. Another remarkable fact is that the results for $N(t)$ depend very smoothly on $\tilde{\gamma}$, since curves corresponding to values of $\tilde{\gamma}$ differing in several orders of magnitude turn out to be almost coincident (see inset). These two facts show the strong diffusion-limited character of the process.

Simulations (for annihilation and trapping reactions) were performed on a lattice of L sites with periodic boundary conditions, where the B particles were fixed in random positions in each realization and the A particles underwent continuous time random walks. When particles of different kinds meet, the corresponding reaction takes place with a probability depending on the reaction rate γ (with probability 1 for a perfect reaction). The A particles are injected at a single site one by one, every $1/n_p$ units of time. A detailed description of

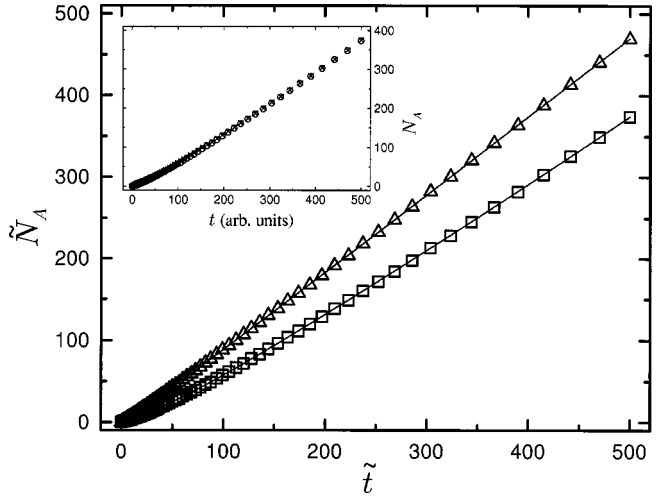

FIG. 5. Temporal evolution of the number of surviving A particles for an annihilation reaction. The solid line corresponds to MF results and the dots correspond to numerical simulations for $D = 2$ (squares) and $D = 0.05$ (triangles). The rest of the parameters are the same as in Fig. 4. The inset shows simulations for the number of particles for $\gamma = 0.1$ (crosses) and $\gamma = \infty$ (circles); the rest of the parameters are the same as those corresponding to squares. The lattice is of 200 sites except for the triangles that is of 100 sites.

the algorithm used can be seen in [11]. All simulations shown in the figures are averages over 100 realizations.

IV. CONCLUSIONS

We have analyzed trapping and annihilation reactions in a one-dimensional substrate where the B particles are fixed and the A particles are injected by a localized source. We have studied in each case the temporal evolution of the number of particles and the density profiles. The appearance of the A particle profiles in both situations is a large growing peak located around the position of the source. The theoretical results of the SM and the MF model were compared with simulations in both situations.

For imperfect trapping reactions we found that the SM gives a much better description than the MF model, as was to be expected. The approximate solutions of the SM correctly describe the simulations up to larger times and, more important, also predict useful scaling relations that are valid at all times.

For perfect trapping reactions we have obtained the exact analytical results of the $n_A(x,t)$ and $N_A(t)$ within the SM (in an infinite lattice) showing excellent agreement with simulations. In addition, by considering a finite lattice we have obtained the stationary behavior for the same quantities. It is worth remarking that the finite-size effects are present even when the tail of the peaked distributions induced by the source does not reach the lattice boundaries.

For imperfect annihilation we have found that the SM gives a good agreement with simulation data. Remarkably, in this case the MF model also provides a reasonable description of the problem, unlike what happens in homogeneous annihilation processes in low-dimensional systems. This is due to the absence of segregation effects. However, segregation would become important if a nonzero initial density of A particles were considered, causing the MF model to fail.

We have found that the system has only two effective parameters, $\tilde{D}=Dn_{B0}^2/n_p$ and $\tilde{\gamma}=\gamma n_{B0}/n_p$; however, the results show a high degree of independence on $\tilde{\gamma}$. Hence, $\tilde{D}$ remains as the only relevant parameter. An important fact worth remarking is that, due to this independence, the results for imperfect reactions become similar to those for a perfect reaction presented in [22]. An experimental realization like the one suggested in the Introduction, would allow us to test the scaling relations by comparing results at different temperatures (that induce changes in the system's parameters), or varying the B reactant concentration or the A pumping rate.

Another interesting point is that the dependence of $n_A(x,t)$ and $N_A(t)$ on n_p is found to be linear for the trapping case (it comes as a general factor), while it is a nontrivial (nonlinear) one for the annihilation case.

Summarizing, we have presented an analysis of the effect of localized sources of A particles on a substrate of B particles confirming the goodness of the stochastic model for describing such situations. Further extensions of these cases are under way.

ACKNOWLEDGMENTS

The authors want to thank V. Grünfeld for a revision of the manuscript. Financial support from CONICET (Project No. PIP-4953/96) and ANPCyT (Project No. 03-00000-00988), Argentina, is acknowledged. A.D.S. thanks the Fundación Antorchas (Project No. A-13579/1-49) for partial financial support.

[1] S. Redner and F. Leyvraz, in *Fractals in Science*, edited by A. Bunde and S. Havlin (Springer-Verlag, Berlin, 1994).
[2] M. V. Smoluchowski, Z. Phys. Chem. **92**, 129 (1917).
[3] S. A. Rice, *Diffusion-Limited Reactions* (Elsevier, Amsterdam, 1985).
[4] G. Abramson, Ph.D. thesis, Instituto Balseiro, Universidad Nacional de Cuyo, Argentina, 1995 (unpublished); A. Bru Espino, Ph.D. thesis, Facultad de Ciencias Físicas, Universidad Complutense de Madrid, Spain, 1995 (unpublished).
[5] M. A. Rodriguez, G. Abramson, H. S. Wio, and A. Bru, Phys. Rev. E **48**, 829 (1993).
[6] G. Abramson, A. Bru Espino, M. A. Rodriguez, and H. S. Wio, Phys. Rev. E **50**, 4319 (1994).
[7] G. Abramson and H. Wio, Chaos Solitons Fractals **6**, 1 (1995); H. S. Wio, G. Abramson, M. A. Rodriguez, and A. Bru, *ibid.* **6**, 575 (1995).
[8] G. Abramson and H. S. Wio, Phys. Rev. E **53**, 2265 (1996).
[9] A. D. Sánchez and H. S. Wio, Physica A **237**, 452 (1997).
[10] M. A. Rodriguez and H. S. Wio, Phys. Rev. E **56**, 1724 (1997).
[11] A. D. Sánchez, M. A. Rodriguez, and H. S. Wio, Phys. Rev. E **57**, 6390 (1998).
[12] A. D. Sánchez, E. M. Nicola, and H. S. Wio, Phys. Rev. Lett. **78**, 2244 (1997).
[13] L. Galfi and Z. Racz, Phys. Rev. A **38**, 3151 (1988); Z. Jiang and C. Ebner, *ibid.* **42**, 7483 (1990).
[14] B. Chopard and M. Droz, Europhys. Lett. **15**, 459 (1991); S. Cornell, M. Droz, and B. Chopard, Phys. Rev. A **44**, 4826 (1991); Physica A **188**, 322 (1992).
[15] Y.-E. Lee Koo and R. Kopelman, J. Stat. Phys. **65**, 893 (1991).
[16] H. Taitelbaum, S. Havlin, J. Kiefer, B. Trus, and G. H. Weiss, J. Stat. Phys. **65**, 873 (1991); H. Taitelbaum, Y.-E. Lee Koo, S. Havlin, R. Kopelman, and G. H. Weiss, Phys. Rev. A **46**, 2151 (1992); E. Ben-Naim and S. Redner, J. Phys. A **25**, L575 (1992).
[17] H. Larralde, M. Araujo, S. Havlin, and H. E. Stanley, Phys. Rev. A **46**, 855 (1993); **46**, R6121 (1992); M. Araujo, S. Havlin, H. Larralde, and H. E. Stanley, Phys. Rev. Lett. **68**, 1791 (1992).
[18] B. Chopard, M. Droz, T. Karapiperis, and Z. Racz, Phys. Rev. E **47**, R40 (1993).
[19] S. J. Cornell, Phys. Rev. Lett. **75**, 2250 (1995); Phys. Rev. E **51**, 4055 (1995).
[20] F. G. Nicolini, M. A. Rodriguez, and H. S. Wio, ICTP Report No. IC/94/161, 1994 (unpublished); M. A. Rodriguez and H. S. Wio, ICTP Report No. IC/94/162, 1994 (unpublished).
[21] B. P. Lee and J. Cardy, Phys. Rev. E **50**, R3287 (1994); J. Stat. Phys. **80**, 971 (1995); M. Howard and J. Cardy, J. Phys. A **28**, 3599 (1995).
[22] H. Larralde, Y. Lereah, P. Trunfio, J. Dror, S. Havlin, R. Rosenbaum, and H. E. Stanley, Phys. Rev. Lett. **70**, 1461 (1993).
[23] *Handbook of Mathematical Functions*, edited by M. Abramowitz and I. A. Stegun (Dover, New York, 1972).